Interference Avoidance Transmission by Partitioned Frequency- and Time-domain Processing

Yasunori Futatsugi and Masayuki Ariyoshi
System Platforms Research Laboratories, NEC Corporation
Kawasaki, Japan
y-futatsugi@cq.jp.nec.com, ariyoshi@bx.jp.nec.com

Abstract— **This paper presents an interference avoidance transmission technique for dynamic spectrum access (DSA). Generally, OFDM transmission induces high out-of-band emission due to the side-lobes of the transmitted sub-carriers. For a DSA based OFDM system, it is thus important to reduce the out-of-band emission. Aiming at providing high suppression effect for an interference avoidance notch, an interference avoidance transmission by partitioned frequency- and time-domain processing (IA-PFT) is proposed. IA-PFT is configured by a partitioned combination of the CC processing in the frequency domain and windowing processing in the time domain. Computer simulations show that IA-PFT reduces the interference power spectrum density under the condition of a highly prioritized wireless microphone in white space. Moreover, it is shown that IA-PFT realizes transmission performance and PAPR performance as much as those attained by conventional interference avoidance methods.**

Keywords - interference suppression; windowing; active interference cancellation; cancellation carrier; dynamic spectrum access

I. INTRODUCTION

It is anticipated that future wireless communication systems will face exhaustion of frequency resources, because expected broadband and various radio services will require more and flexible frequency resources. Dynamic spectrum access (DSA) has recently attracted attention as a promising cognitive radio [1] technology for improving frequency spectrum utilization. DSA can allow a low-priority system to transmit on the shared spectrum without causing harmful interference to high-priority system. For example, the low-priority system may notch the highly-prioritized bandwidth out from its transmit spectrum to avoid interference. In the case of orthogonal frequency division multiplexing (OFDM)-based transmission, undesired spectrum emission is induced by high power side-lobes of the transmitted sub-carriers. For a low-prioritized OFDM-based DSA system, it is important to reduce the undesired out-of-band spectrum emission so that the system can coexist with high-priority system. A windowing technique in the time domain is used in IEEE802.11a [2], which is referred to as time windowing (TW). TW is able to significantly reduce out-of-band emission for the center of the notch. Alternatively, active interference cancellation (AIC) is known as a method of inserting interference suppression carriers into the original transmission sub-carriers to suppress the side-lobes in the interference avoidance notch [3]. Similar approaches, called as cancellation carrier (CC) insertion [4] have been studied (In this present paper, the CC insertion is considered as a kind of AIC). The CC insertion is able to significantly reduce out-of-band emission at the edge of the notch. A simple serial combination of CC insertion and TW has been investigated in [5]. However, this approach cannot achieve enough synergy of the combination of CC insertion and TW, because the suppression effect by CC insertion at the edge is insufficient due to a cyclic extension in TW processing.

Aiming at achieving deep suppression in the entire notch, we propose an interference avoidance transmission by partitioned frequency- and time-domain processing (called as IA-PFT hereafter) for DSA, which synergizes combination effect of CC and TW. IA-PFT is configured by partitioned a combination of the CC insertion in the frequency domain and TW processing in the time-domain: that is, the CC insertion and TW are separately applied to the transmitted sub-carriers. Hence, the suppression effect by CC insertion is not violated by the TW. For adequate synergy effect of TW and CC insertion, the proposed IA-PFT allocates the sub-carriers suppressed by the CC near the notch. Furthermore, the proposed IA-PFT employs TW to the rest of the sub-carriers. It is shown that the proposed IA-PFT can achieve high suppression effect for the entire band of the notch. Moreover, IA-PFT realizes transmission performance and PAPR performance as good as those attained by conventional interference avoidance methods. Computation complexities are also analyzed for those interference avoidance transmission methods.

The organization of this paper is as follows. Section II describes the method of the proposed IA-PFT. Section III presents the fundamental analysis on side-lobe suppression by cancellation carrier-based techniques. Section IV provides the results obtained by computer simulations to evaluate the performance of the proposed IA-PFT. Finally, concluding remarks are made in Section V.

978-1-4673-0990-5/12/$31.00 ©2012 IEEE

II. Interference Suppression Technique By Partitioned Frequency-And Time-Domain

A. Transmitter Structure

In this paper, it is assumed that the low-priority system exploits both of the exclusive band and the shared band [6]. We focus on the FFT/IFFT processing scheme for the shared band on a multi-RF transmitter [7]. Figure 1 shows the transmitter structure of IA-PFT. The transmitter employs a twin-IFFT scheme for the shared band transmitted signal. The transmitted bit stream is modulated and divided into a time-windowing-processed signal stream and a CC-processed signal stream at the sub-carrier mapping. A cyclic prefix and a cyclic postfix (commonly abbreviated as CP) are respectively appended to the head of the OFDM symbols and to the tail of the OFDM symbols [2]. The reason for appending the CPs is to smooth the OFDM symbols without shaping original rectangular OFDM symbols to avoid signal distortion. As for the CC-processed signal stream, CCs are inserted into the original transmitted sub-carriers in the frequency domain to suppress undesired spectrum emission near the edge of notch. A ZP is appended to the head of the OFDM symbols. The reason of the ZP appendix is to match the side-lobes of the CCs and those of the transmission sub-carriers, and consequently to enhance suppression effect by CC insertion.

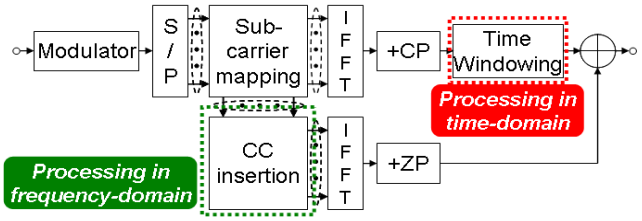

Figure 1. Transmitter structure

B. Transmission Method

Figure 2 shows the sub-carrier allocation of IA-PFT. CCs are inserted close to the interference avoidance notch (N_i). The CCs are calculated to suppress side-lobes on a null band ($N_{i\_partial}$) from the interference sources covered by the CC-processed signal (Q sub-carriers). The null band is set to the vicinity of the CCs in the notch. Aiming at achieving adequate synergy effect of TW and CC insertion, the sub-carriers of the low-priority system suppressed by the CCs are allocated near the CCs, and the rest of the sub-carriers for the low-priority system are suppressed by the TW.

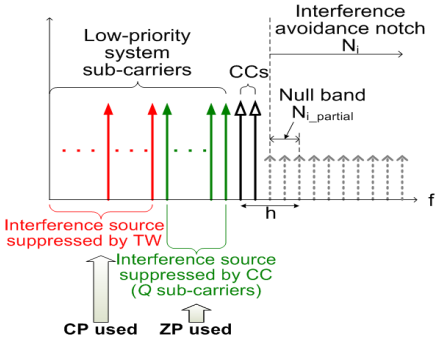

Figure 2. Sub-carrier allocation

The interference-suppressed signal $x(r)$ is expressed as

$$x(r) = x_{CC}(r) + x_{TimeWindowing}(r) \tag{1}$$

where $x_{CC}(r)$ and $x_{TimeWindowing}(r)$ are respectively the CC-processed signal and the time-windowing-processed signal. The index r (where r=0, 1, 2,…, $N+L_{CP}+L_{OV}-1$, where N is FFT size, L_{CP} is the length of a cyclic prefix and a ZP, and L_{OV} is the overlapping sample for the TW which equals to the length of a cyclic postfix) is the sample.

The CC-processed signal is expressed as

$$x_{CC}(n) = \sum_{k=0}^{N-1} X'(k) \exp\left(j2\pi \frac{nk}{N}\right) \tag{2}$$

where $X'(k)$ is the transmitted symbol with CC vector. The indices n (n=0, 1, 2,…, N-1) and k (k=0, 1, 2,…, N-1) are respectively the sample and the sub-carrier.

The transmitted symbol vector with CC vector, $\mathbf{X}'$, can be obtained by inserting CC vector $\mathbf{h}$ [3] to the CC-processed symbol vector $\mathbf{X}$. The CC vector $\mathbf{h}$ is expressed as

$$\mathbf{h} = -\left(\mathbf{P}_1^T \mathbf{P}_1\right)^{-1} \mathbf{P}_1^T \mathbf{P}_S \mathbf{X} \tag{3}$$

where $\mathbf{P}_s$ is the matrix of the extraction of the matrix $\mathbf{P}$ corresponding to the side-lobes on the null band after up-sampling, and $\mathbf{P}_1$ is the extraction of the matrix $\mathbf{P}_s$ corresponding to the null band including the CC vector. The equation (3) is based on a minimum mean-squared error solution. The length of the CC vector, $\mathbf{h}$, represents $N_{i\_partial}+N_{CC}$ (where $N_{i\_partial}$ is the length of the null band, and N_{CC} is the length of CC vector). Matrix $\mathbf{P}$ consists of the conversion function $P(l,k)$ [3] expressed as

$$P(l,k) = \sum_{n=0}^{N-1} \exp\left(j2\pi \frac{n}{N}\left(k - \frac{l}{M}\right)\right) \tag{4}$$

where l and M are respectively the up-sampled frequency position and the up-sampling ratio for the CC calculation.

The time-windowing-processed signal $x_{TimeWindowing}(r)$ is expressed as

$$x_{TimeWindowing}(r) = g(r)x(r) \tag{5}$$

where $g(r)$ and $x(r)$ are respectively the shaping coefficient for the TW and the OFDM symbol accompanying the CPs. The shaping coefficient is based on a raised cosine roll-off characteristic.

The shaping coefficient $g(r)$ is given as

$$g(r) = \begin{cases} \frac{1}{2} + \frac{1}{2}\cos\left(\pi + \frac{\pi r}{L_{OV}}\right) & ,0 \le r < L_{OV} \\ 1 & ,L_{OV} \le r < L_{CP} + N \\ \frac{1}{2} + \frac{1}{2}\cos\left(\frac{\pi(r - (L_{CP} + N))}{L_{OV}}\right) & ,L_{CP} + N \le r < L_{CP} + N + L_{OV} \end{cases} \tag{6}$$

III. FUNDAMENTAL ANALYSIS ON SIDE-LOBE SUPPRESSION BY CANCELLATION CARRIER-BASED TECHNIQUES

This section presents a fundamental analysis on the side-lobe suppression by CC insertion techniques [3][4], the simple serial combination of the CC insertion and TW [5], and IA-PFT. The frequency spectrum of k-th sub-carrier for CC insertion is expressed as

$$S'_k(f) = X'(k)\frac{\sin(\pi(f-f_k)T_s)}{\pi(f-f_k)T_s} \qquad (7)$$

where T_s is the OFDM symbol duration of N sample. The indices f and f_k are respectively the frequency and the carrier frequency of the k-th sub-carrier [5]. The sub-carrier spacing equals to $\Delta f = 1/T_s$. The frequency spectrum of k-th sub-carrier for TW is expressed as

$$S_k(f) = X(k)\frac{\sin(\pi(f-f_k)T_o)}{\pi(f-f_k)T_o} \qquad (8)$$

where T_o is the OFDM symbol duration of N + L_{CP} sample. Although the sub-carrier spacing equals to $\Delta f = 1/T_s$ for TW, the pitch of side-lobes is shortened by the cyclic extension. This implies that peak positions of side-lobes do not match in frequency domain and have negative impact on the suppression effect of CC insertion. To clarify the effect of the CC insertion, power spectrum densities in the null band ($N_{i\_partial}$) were analyzed. Figure 3 shows the transmission spectrum image produced by the CC insertion. The average power spectrum density is about –32 dB in the null band. The CC insertion can achieve high suppression effect in the null band. It can be seen that the side-lobes of the transmission sub-carriers and those of CCs match in the frequency domain. The reason for this matching is that the ZP is appended to each OFDM symbol instead of the CP. Figure 4 shows the transmission spectrum image produced by the simple serial combination of the CC insertion and TW. In this analysis, the N_{CC}, $N_{i\_partial}$ and L_{OV} were respectively set to 2, 3 and 30. The CP is appended to all the transmission subcarriers. The average power spectrum density is about –25 dB in the null band. This result indicates that the interference suppression effect obtained by the simple serial combination of the CC insertion and TW is not high in the null band for this system model. Less suppression effect is induced by the unmatched side-lobes of the transmission sub-carriers and those of CC vector in the frequency domain. This is caused by cyclic extension of the OFDM symbols used in the TW processing. Figure 5 shows the transmission spectrum image produced by IA-PFT. The parameter Q was set to 15 for IA-PFT. The average power spectrum density is about –30 dB in the null band. It can be seen that the suppression effect is almost same as that of the CC insertion. The side-lobes of Q sub-carriers and those of CC vector match in the frequency domain. On the other hand, the side-lobes of the sub-carriers suppressed by the TW become extremely low power level, because those sub-carriers are allocated in far frequency position from the null band. The analysis results thus imply that the suppression effect of IA-PFT improves compared to that of the simple serial combination of the CC insertion and TW.

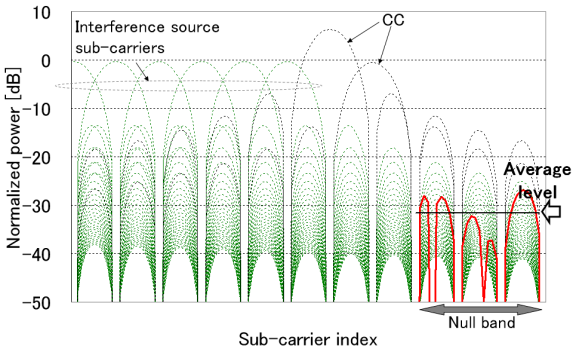

Figure 3. Transmission spectrum of CC insertion (ZP appended to each sub-carrier)

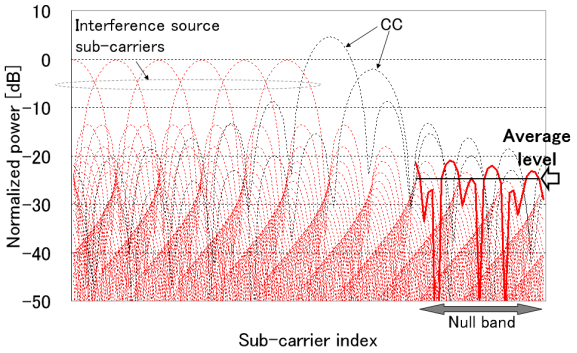

Figure 4. Transmission spectrum of simple serial combination of CC insertion and TW (CP appended to each sub-carrier)

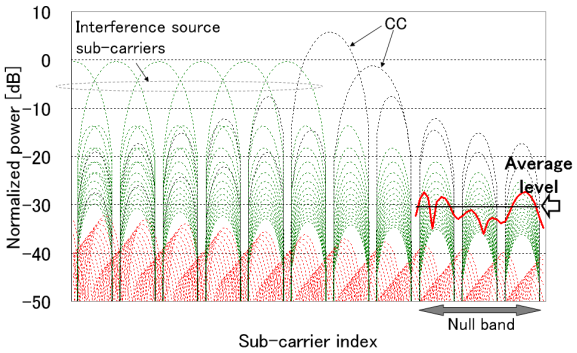

Figure 5. Transmission spectrum of IA-PFT (CP and ZP appended to each sub-carrier)

IV. PERFORMANCE EVALUATION

The interference suppression effect of IA-PFT was evaluated by computer simulations. The following section presents the evaluation results on power spectrum density, transmission performance, PAPR and computational complexity. These evaluations covered actual-use cases such as interference avoidance for wireless microphone.

A. Simulation Parameters

The major parameters (based on 3GPP Evolved UTRA [8][9]) used in the simulation are listed in Table 1.

TABLE I. SIMULATION PARAMETERS

Parameter	*Assumption*
FFT size	1024
Number of effective sub-carriers	564
Cyclic prefix (ZP) sample	72
Sub-carrier spacing	15 kHz
Channel coding / decoding	Turbo coding (K=4) / Max-Log-MAP decoding
Modulation scheme	QPSK, 16QAM (R= 3/4)
Channel model	Typical Urban
Maximum Doppler frequency	f_D=20 Hz
Channel estimation	Ideal
Number of receiver antennas	2

B. *Evaluation on Power Spectrum Density for Wireless Microphone*

It is assumed that a wireless microphone is a high-priority system. Such wireless microphones (e.g., PMSE devices) are used in the white space of the digital terrestrial TV (DTV) band in Europe. If a low-priority system utilizes the white space of DTV, interference avoidance is required. Figure 6 shows an overview of the interference avoidance behavior for the wireless microphone. The assumed bandwidth of the wireless microphone is 200 kHz. The bandwidth of resource block (RB) of the low-priority system is 180 kHz [9]. In this case, the 3 RBs are not transmitted per active wireless microphone channel.

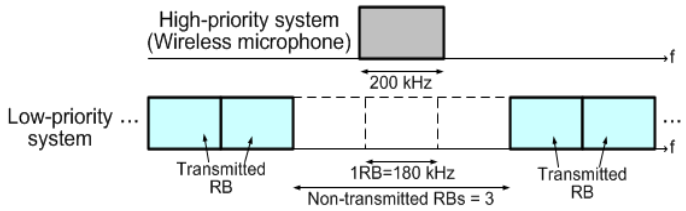

Figure 6. Overview of interference avoidance behavior for wireless microphone

Figure 7 shows the transmission spectrum in the case of the interference avoidance for the wireless microphone under the same condition as that of Figure 6. In the figure, the performance of IA-PFT is compared with those of the normal OFDM, TW, CC insertion and the serial combination of CC insertion and TW (shown as CC+TW serial). The number of sub-carriers for the notch (N_i) was set to 32. For the TW, the number of sub-carriers for the notch was set to 34 to fit the same spectrum efficiency of the CC insertion and IA-PFT. As for IA-PFT, interference suppression partitioned by the CC insertion and TW was applied to each spectrum edge. N_{CC}, $N_{i\_partial}$, L_{OV} and Q were respectively set to 2, 3, 30 and 15. QPSK modulation scheme was assumed. From the simulation results, the TW and CC+TW serial cannot achieve the high suppression effect near the transmitted sub-carriers in the notch. Meanwhile, the CC insertion cannot achieve the high suppression effect in the central portion of the notch. For IA-PFT, the maximum suppression effect of power spectrum density is about 10 dB higher than attained by the CC+TW serial. Furthermore, IA-PFT can obtain the maximum suppression effect of 14 dB compared with the normal OFDM.

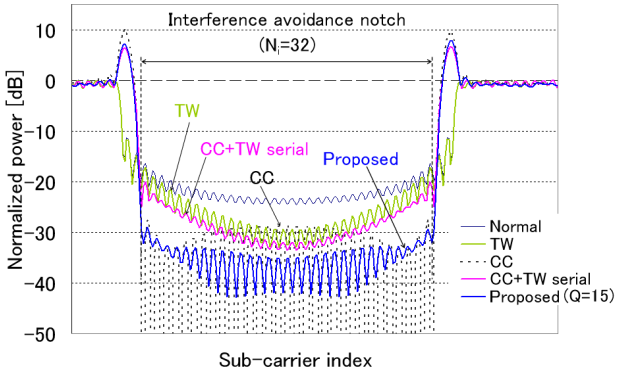

Figure 7. Transmission spectrum of notch for wireless microphone

Figure 8 shows the transmission spectrum for IA-PFT when the number of sub-carriers processed by CC (Q) is changed. If the Q is set to a smaller value, the spectrum of IA-PFT reaches that of TW. On the other hand, if the Q is set to a larger value, the spectrum of IA-PFT reaches that of CC insertion. This result indicates that IA-PFT spectrum can be controlled by changing the parameter Q.

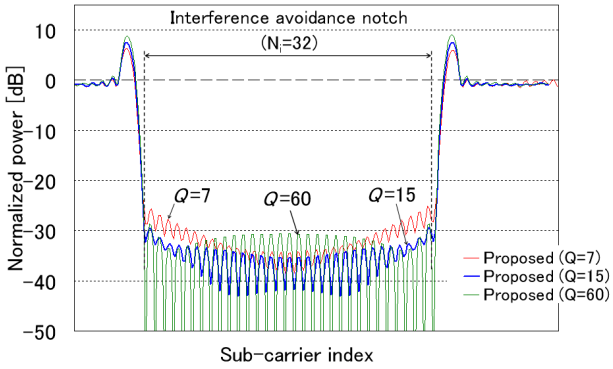

Figure 8. Transmission spectrum of notch for wireless microphone (variable Q for IA-PFT)

C. *Transmission Performances in Multi-Path Fading Channels*

Figure 9 shows the block-error-rate (BLER) performance of IA-PFT with a condition of coding rate of 3/4 (R=3/4) and four notches (i.e., the number of notches, N_{notch}, equals to 4). This is a kind of severe conditions for IA-PFT such as higher coding rate and multiple active channels used by wireless microphone. As comparison methods, the CC, TW and CC+TW serial were also evaluated. The required E_b/N_0 at BLER of 10^{-2} for IA-PFT is almost same as that in the case of the TW and CC+TW serial. However, the BLER performance of the CC is worse than that of IA-PFT, because the inter-carrier-interference (ICI) is induced by the ZP. The difference between transmission performance of IA-PFT and of the TW is 0.1 dB in the case of 16QAM. This performance impairment for IA-PFT is caused by the ZP appended sub-carriers. Nevertheless, the loss of the required E_b/N_0 can be seen as small because the maximum suppression effect attained by 12 dB compared to that of the TW.

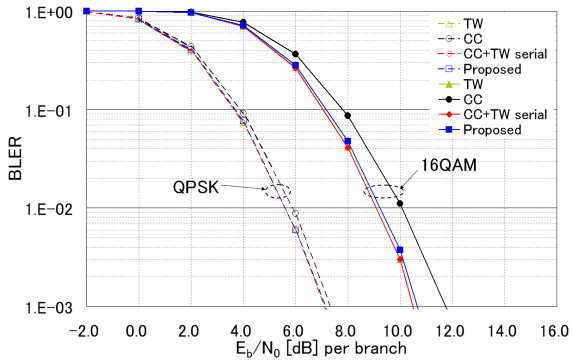

Figure 9. Transmission performance (R=3/4, N_{notch}=4)

D. *PAPR Performances*

Figure 10 shows PAPR of IA-PFT when 16QAM, R=3/4 and N_{notch}=4 are assumed. In this evaluation, the simulation parameters were set to same values as Figure 9. From the simulation result, PAPR of CC insertion is increased by 0.4 dB compared to the TW when Complementary Cumulative Distribution Function (CCDF) is equivalent to 1%. The reason of the increase of PAPR for CC insertion is that ZP is used for all the sub-carriers. On the other hand, PAPR of IA-PFT is almost same as that of the TW since ZP is partially used for the sub-carriers.

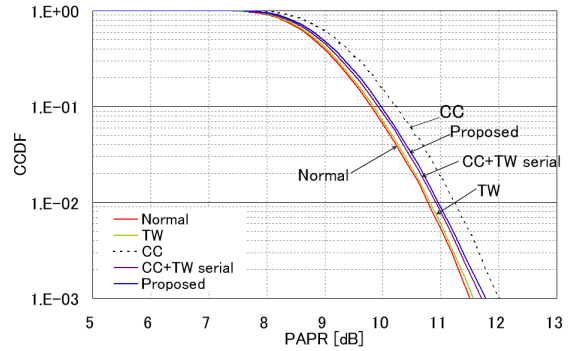

Figure 10. PAPR (16QAM, R= 3/4, N_{notch}=4)

E. *Computational complexity*

For the transmitter side of IA-PFT, additional complexity is required due to twin-IFFT scheme. The number of multiplications per OFDM symbol is expressed as

$$\mu_{IA-PFT}^{Tx} = N\log_2 N + 2L_{OV} + N_{CC}N_{edge}Q \quad (9)$$

where N , L_{OV} , N_{CC} , N_{edge}, and Q are respectively FFT size, the number of overlapping samples for TW, the number of CCs, the number of spectrum edges, and the number of sub-carriers processed by CC. The complexity analysis result is listed in Table 2. It is defined that $N_{effective}$ represents the number of effective sub-carriers. The complexity of IA-PFT increases compared with that of TW. However, it can be seen that the increase of complexity is not high if all of the baseband processing is considered. It is also noted that a normal OFDM receiver can be used for IA-PFT receiver which does not require any interference cancellation processing.

TABLE II. COMPLEXITY ANALYSIS

Transmission scheme	*Complexity*
NC-OFDM	$\mu_{NC}^{Tx} = \frac{N}{2}\log_2 N$
TW	$\mu_{TW}^{Tx} = \frac{N}{2}\log_2 N + 2L_{OV}$
CC	$\mu_{CC}^{Tx} = \frac{N}{2}\log_2 N + N_{CC}N_{edge}N_{effective}$
CC+TW serial	$\mu_{CC+TW}^{Tx} = \frac{N}{2}\log_2 N + 2L_{OV} + N_{CC}N_{edge}N_{effective}$
IA-PFT	$\mu_{IA-PFT}^{Tx} = N\log_2 N + 2L_{OV} + N_{CC}N_{edge}Q$

V. CONCLUSIONS

A novel interference suppression method called IA-PFT was proposed. The structure of IA-PFT features a combination of parallel processing of transmit sub-carriers in frequency domain (CC insertion) and in time domain (TW). IA-PFT allocates the sub-carriers suppressed by the CCs near the notch. This contributes to achieve high suppression effect near the edge of the notch. Besides, IA-PFT applies the TW to the rest of the sub-carriers. This contributes to achieve high suppression effect at the center of notch. Computer simulations showed that IA-PFT outperforms the conventional methods in terms of interference suppression effect. Moreover, negative impacts of IA-PFT on transmission performance and PAPR performance are low enough. Complexity analysis result was also presented. It is therefore concluded that IA-PFT is a promising candidate for OFDM-based DSA systems.

ACKNOWLEDGMENT

The research leading to these results was derived from the European Community's Seventh Framework Programme (FP7) under Grant Agreement number 248454 (QoSMOS).

REFERENCES

[1] J. Mitola III and G.Q. Maguire Jr., "Cognitive radio: making software radios more personal," *IEEE Personal Commun.*, vol.6, no.4, pp.13–18, Aug. 1999.

[2] IEEE, "Supplement to IEEE Standard for Information technology—Telecommunications and information exchange between systems—Local and metropolitan area networks—Specific requirements—Part 11: Wireless LAN Medium Access Control (MAC) and Physical Layer (PHY) specifications: High-speed Physical Layer in the 5 GHZ Band", IEEE Std 802.11a-1999.

[3] H. Yamaguchi, "Active interference cancellation technique for MB-OFDM cognitive radio," *Microwave conference2004*, pp.1105–1108, Oct. 2004.

[4] S. Brandes, I. Cosovic and M. Schnell, "Sidelobe suppression in OFDM systems by insertion of cancellation carriers," *VTC2005-Fall*, pp.152–156, Sept. 2005.

[5] S. Brandes, I. Cosovic and M. Schnell, "Reduction of out-of-band radiation in OFDM based overlay systems," *DySPAN2005*, pp.662–665, Nov. 2005.

[6] Y. Sagae and H. Yoshino, "Performance evaluation of a spectrum sharing method with joint power control and spectrum aggregation techniques," *IEICE technical report*, SR2008–71, Jan. 2009 (in Japanese).

[7] S. Sampei, S. Miyamoto and S. Ibi, "Spectrum loading type dynamic spectrum allocation technique for cognitive radio systems," *CROWNCOM2007*, pp.535–539, Aug. 2007.

[8] 3GPP, TS 36.201 (V9.1.0), "LTE Physical Layer - General Description," Mar. 2010.

[9] 3GPP, TS 36.211 (V9.1.0), "Physical channels and modulation," Mar. 2010.